THE JOURNAL OF BIOLOGICAL CHEMISTRY VOL. 287, NO. 40, pp. 33745–33755, September 28, 2012


# Loss- and Gain-of-function PCSK9 Variants

## *CLEAVAGE SPECIFICITY, DOMINANT NEGATIVE EFFECTS, AND LOW DENSITY LIPOPROTEIN RECEPTOR (LDLR) DEGRADATION*[*] [S]

Received for publication, July 10, 2012, and in revised form, August 2, 2012 Published, JBC Papers in Press, August 8, 2012, DOI 10.1074/jbc.M112.399725

**Suzanne Benjannet**[‡], **Josée Hamelin**[‡], **Michel Chrétien**[§¶1], **and Nabil G. Seidah**[‡2]

*From the* [‡]*Laboratory of Biochemical Neuroendocrinology,* [§]*Clinical Research Institute of Montreal, University of Montreal, 110 Pine Avenue West, Montreal, Quebec H2W1R7, Canada and* [¶]*Ottawa Hospital Research Institute, 725 Parkdale Avenue, Ottawa, Ontario K1Y4E9, Canada*

**Background:** Autocatalytic zymogen processing of pro-PCSK9 requires cleavage at $Gln^{152}\downarrow$.
**Results:** Only a few residues can replace $Gln^{152}$ without loss of function. Non-favorable residues result in a dominant negative zymogen retaining intracellularly native pro-PCSK9. A wide variety of $Asp^{374}$ gain-of-function mutations were characterized.
**Conclusion:** Zymogen processing is necessary for secretion. Its inhibition results in a dominant negative protein.
**Significance:** A novel strategy for PCSK9 inhibition is suggested.

**The proprotein convertase PCSK9 is a major target in the treatment of hypercholesterolemia because of its ability bind the LDL receptor (LDLR) and enhance its degradation in endosomes/lysosomes. In the endoplasmic reticulum, the zymogen pro-PCSK9 is first autocatalytically cleaved at its internal $Gln^{152}\downarrow$, resulting in a secreted enzymatically inactive complex of PCSK9 with its inhibitory prosegment (prosegment·PCSK9), which is the active form of PCSK9 on the LDLR. We mutagenized the P1 cleavage site $Gln^{152}$ into all other residues except Cys and analyzed the expression and secretion of the resulting mutants. The data demonstrated the following. 1) The only P1 residues recognized by PCSK9 are Gln > Met > Ala > Ser > Thr ≈ Asn, revealing an unsuspected specificity. 2) All other mutations led to the formation of an unprocessed zymogen that acted as a dominant negative retaining the native protein in the endoplasmic reticulum. Analysis of a large panoply of known natural and artificial point mutants revealed that this general dominant negative observation applies to all PCSK9 mutations that result in the inability of the protein to exit the endoplasmic reticulum. Such a tight quality control property of the endoplasmic reticulum may lead to the development of specific PCSK9 small molecule inhibitors that block its autocatalytic processing. Finally, inspired by the most active gain-of-function mutant, D374Y, we evaluated the LDLR degradation activity of 18 $Asp^{374}$ variants of PCSK9. All $Asp^{374}$ mutations resulted in similar gain-of-function activity on the LDLR except that D374E was as active as native PCSK9, D374G was relatively less active, and D374N and D374P were completely inactive.**

Mammalian genomes encode nine secretory proprotein convertases (PCs)[3] related to bacterial subtilisin and yeast kexin (1–3). Seven of them, PC1/3, PC2, furin, PC4, PC5/6, PACE4, and PC7, cleave precursors at single or pairs of basic amino acids, and the last two convertases, SKI-1/S1P and PCSK9, cleave at non-basic sites.

The last member, PCSK9, discovered in 2003 (4) turned out to have a major role in regulating cholesterol homeostasis by increasing the levels of circulating low density lipoprotein cholesterol (5). The underlying mechanism involves the ability of PCSK9 to bind to and enhance the degradation of the hepatic LDL receptor (LDLR) (6) in acidic subcellular compartments (7, 8), likely endosomes/lysosomes (9). Early biosynthetic analyses revealed that this enzyme is synthesized as a zymogen (pro-PCSK9) in the endoplasmic reticulum (ER) that is autocatalytically activated (4) through cleavage at the C terminus of its inhibitory prosegment, *i.e.* at the $VFAQ^{152}\downarrow$ sequence (8, 10). As is the case for most other PCs (1, 2), such zymogen cleavage allows PCSK9 to exit from the ER as a complex with its prosegment. However, different from the other PCs, the inhibitory prosegment remains permanently bound to the catalytic subunit of the secreted PCSK9 as a prosegment·PCSK9 complex (4, 8), keeping it in a catalytically inactive state (11). This unusual behavior for a PC (1) suggested that either the prosegment is removed under certain cellular conditions, thereby releasing the active enzyme, or that the enzymatic activity of PCSK9 is not necessary for its ability to promote the degradation of the LDLR. The validation of the latter hypothesis on three PCSK9 targets, namely the LDLR (12, 13), VLDL receptor, and ApoER2 (14), confirmed that PCSK9 acts non-enzymatically on these receptor targets.

The enzymatically dead form of the secreted PCSK9 precluded the study of its catalytic preference on substrates other than itself. Only a single study revealed that mutation of the P1

* This work was supported by Canadian Institutes of Health Research (CIHR) Grant MOP-102741, Team Grant MOP-44363, and Canada Chair Grant 216684 (to N. G. S.), CIHR Grants MOP-102618 and 211351 (to M. C.), and Strauss Foundation grants (to N. G. S. and M. C.).
[S] This article contains supplemental Figs. S1–S3 and Tables S1 and S2.
[1] Research emeritus professor of the Clinical Research Institute of Montreal.
[2] To whom correspondence should be addressed: Laboratory of Biochemical Neuroendocrinology, Clinical Research Inst. of Montreal, 110 Pine Ave. W., Montreal, Quebec H2W 1R7, Canada. Tel.: 514-987-5609; E-mail: seidahn@ircm.qc.ca.

[3] The abbreviations used are: PC, proprotein convertase; CHRD, cysteine-histidine rich domain; ER, endoplasmic reticulum; GOF, gain-of-function; LDLR, LDL receptor; LOF, loss-of-function; PCSK9, proprotein convertase subtilisin kexin type 9; RFP, red fluorescent protein; Tricine, *N*-[2-hydroxy-1,1-bis(hydroxymethyl)ethyl]glycine; Xbp-1, X-box-binding protein 1.

cleavage site $Gln^{152}$ into Ala still allowed the enzyme to exit the cell, suggesting that PCSK9 may have a relaxed specificity pocket (8), but the activity of the secreted mutant protein on LDLR was not studied. In 2011, Mayne *et al.* (15) published a seminal work on the analysis of the mechanism behind a hypocholesterolemia phenotype observed in a French-Canadian family. The report showed that these subjects harbored a novel Q152H mutation at the autocatalytic P1 $Gln^{152}$ site of wild type (WT) PCSK9. Biosynthetic analysis of this mutant showed two unique results. 1) The presence of a $His^{152}$ instead of the WT $Gln^{152}$ abrogated the ability of pro-PCSK9 to autocatalytically cleave itself in the ER, and 2) the zymogen pro-PCSK9-$His^{152}$ remained in the ER and acted as a dominant negative, preventing the exit of a co-expressed WT form of PCSK9. The net result was that the level of secreted WT PCSK9 was drastically reduced in the presence of this loss-of-function (LOF) natural mutation. This rationalized the low level of circulating PCSK9 in these subjects and their hypocholesterolemia phenotype (15).

In view of the clinical importance of inhibiting PCSK9 for controlling hypercholesterolemia, a number of research laboratories in collaboration with pharmaceutical companies recently reported very encouraging Phase I and II clinical trials using inhibitory monoclonal antibodies or antisense oligonucleotides (2, 16). So far, no small molecule inhibitor has been reported to block the function of PCSK9 likely because of the flat surface of interaction between the catalytic domain of PCSK9 and the EGF-A domain of the LDLR (17, 18).

Finally, biochemical and cellular analyses revealed that the gain-of-function (GOF) D374Y mutation originally observed by Timms *et al.* (19) results from a 10–25-fold higher affinity of PCSK9 for the LDLR (11, 20, 21). This is the most damaging GOF mutation of PCSK9, leading to severe hypercholesterolemia and early death from premature coronary heart disease (22). Although the activities of a few other $Asp^{374}$ artificial mutations were reported (20, 23), they did not cover the spectrum of all amino acids, and their effects on cellular LDLR were not investigated.

We herein characterized the pro-PCSK9 zymogen activation and analyzed the functional consequence on LDLR degradation of all $Gln^{152}$ mutants and a wide variety of LOF mutants. Furthermore, we also present comparative data on the critical importance of $Asp^{374}$ and all its possible mutants in regulating the function of PCSK9 on LDLR.

## EXPERIMENTAL PROCEDURES

*Plasmids and Reagents*—Human PCSK9 and its various mutant cDNAs were cloned into pIRES2-EGFP (Clontech) as described (4). The DsRed2 encoding a red fluorescent protein (RFP) (Clontech) was fused in phase to the C terminus of PCSK9, resulting in the PCSK9-RFP chimera. We also used a PCSK9 construct in which a V5 tag was inserted between the signal peptide (amino acids 1–30) and the start of the prosegment (amino acids 31–152), generating a V5-pro-PCSK9 construct (14). The sequences of all constructs were confirmed by DNA sequencing.

*Cell Culture and Transfections*—HEK293 cells (American Type Culture Collection) were routinely cultivated in Dulbecco's modified Eagle's medium (DMEM; Invitrogen) supplemented with 10% fetal bovine serum (Invitrogen) and maintained at 37 °C under 5% $CO_2$. At 60% confluence, HEK293 cells were transiently transfected in 10-$cm^2$ dishes (0.5 $\mu$g of cDNAs) with Effectene (Qiagen) according to the manufacturer's instructions.

*Biosynthetic Analyses and Immunoprecipitations*—HEK293 cells were transiently transfected as described above. At 48 h post-transfection, the cells were washed in Cys/Met-free RPMI 1640 medium containing 0.2% BSA and pulse-labeled for 3 or 4 h with 250 $\mu$Ci/ml [$^{35}$S]Met/Cys (PerkinElmer Life Sciences). After the pulse, the media were recovered, and the cells were lysed as reported (24). The media and cells lysates were immunoprecipitated with the monoclonal antibodies mAb-V5, or mAb-$His_6$ or with an in house rabbit polyclonal PCSK9 antibody (9). The immunoprecipitated proteins were resolved by SDS-PAGE on 8% Tricine gels, dried, and autoradiographed as described (24).

*Western Blot Analyses*—Cells were lysed in ice-cold radioimmunoprecipitation assay buffer (50 mM Tris-HCl, pH 7.8, 150 mM NaCl, 1% Nonidet P-40, 0.5% sodium deoxycholate, 0.1% SDS) containing a mixture of protease inhibitors (Roche Applied Science). Proteins were analyzed by SDS-PAGE on an 8% Tricine gel. Following the addition of a reducing Tricine sample, solubilized proteins were separated by SDS-PAGE on an 8% Tricine gel. Proteins were visualized using V5-horseradish peroxidase (HRP), PCSK9-HRP, or RFP-HRP and revealed by enhanced chemiluminescence. Quantitation of band intensity was done with Scion Image software from the Scion Corp. (Frederick, MD).

*Reverse Transcription-PCR (RT-PCR) Analysis of X-box-binding Protein 1 (Xbp-1) Splicing*—HEK293 cells were transfected with empty pIRES vector, WT PCSK9, or its Q152A, Q152H, and Q152W mutants alone or together. Forty-eight hours post-transfection, the cells were treated for 4 h with buffer or 5 $\mu$g/ml tunicamycin to induce ER stress. The cells were then lysed, and total RNA was collected (TRIzol®, Invitrogen) as recommended by the manufacturer. Typically, 250 ng of total RNA were used for cDNA synthesis in a total volume of 20 $\mu$l using SuperScript II reverse transcriptase, 25 $\mu$g/ml oligo$(dT)_{12-18}$, 0.5 mM 2′-deoxynucleoside 5′-triphosphates, and 40 units of RNaseOUT, all products from Invitrogen and used according to the recommendations of the manufacturer. Primers used to amplify the Xbp-1 cDNA bearing the intron target of IRE1$\alpha$ ribonuclease activity and PCR conditions were described previously (25). A 289-bp amplicon was generated from unspliced Xbp-1, whereas a 263-bp amplicon was generated from spliced Xbp-1. Four-hour treatment of non-transfected cells with 5 $\mu$g/ml tunicamycin was used as a control for ER stress (26).

*FACS*—HuH7 cells were incubated for 4 h or overnight at 37 °C with various PCSK9 constructs and then washed three times with calcium/magnesium-free Dulbecco's PBS containing 0.5% bovine serum albumin (Sigma) and 1 g/liter glucose (solution A). Cells were then incubated for 5 min at 37 °C with 500 $\mu$l of 1× Versene solution (Invitrogen) and layered on 4 ml of solution A. Cells were then centrifuged for 5 min at 1,200 rpm and resuspended in 1 ml of solution A containing a 1:100

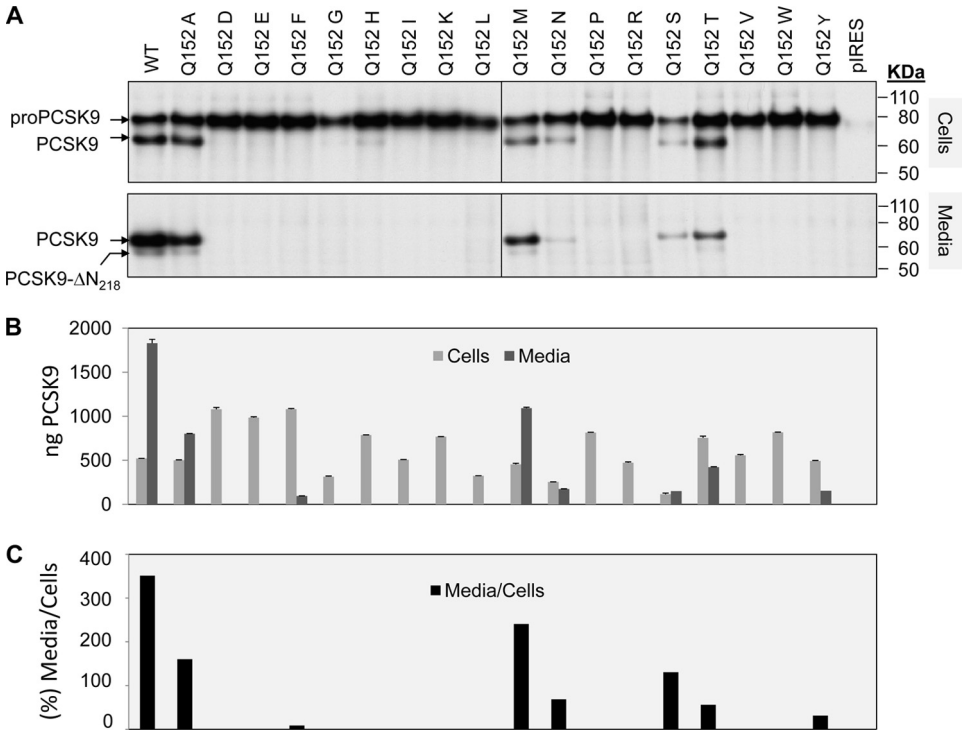


FIGURE 1. **Short term expression and secretion of PCSK9 Gln$^{152}$ mutants.** HEK293 cells were transiently transfected with WT PCSK9-V5 and its Gln$^{152}$ mutants. *A*, 48 h post-transfection, the cells were radiolabeled for 3 h with [$^{35}$S]Met/Cys. The media and cell lysates were then immunoprecipitated with mAb-V5, the immune complexes were resolved by SDS-PAGE on an 8% polyacrylamide Tricine gel, and the dried gel was autoradiographed. The migration positions of pro-PCSK9 and PCSK9 as well as that of the furin-cleaved form, PCSK9-ΔN$^{218}$, are shown. *B*, 24 h post-transfection, cells were washed and incubated for another 24 h in RPMI 1640 medium + 5% lipoprotein-deficient serum. PCSK9 in the media and cell lysates was then quantitated by ELISA. *C*, calculated percent ratio of PCSK9 in media/cells. This figure is representative of three independent experiments done in triplicate. The *error bars* above the mean value represent the range of values ± standard deviation from the mean.

dilution of monoclonal LDLR antibody C7 directed against human LDLR (mAb-C7, Santa Cruz Biotechnology) for 40 min. Cells were washed once with 4 ml of solution A, centrifuged, and resuspended for 20 min in 1 ml of solution A containing a 1:250 dilution of Alexa Fluor 647 donkey anti-mouse IgG (Molecular Probes). Cells were washed and resuspended in 150 $\mu$l of PBS with 0.2% propidium iodide. Viable cells (propidium iodide-negative) were then analyzed by FACS for both propidium iodide and Alexa Fluor 647 using the FACS BD LSR flow cytometer (BD Biosciences).

## RESULTS

*Importance of Gln$^{152}$ in the Zymogen Processing of Pro-PCSK9 and the Dominant Negative Effects of Its Mutants*—We first wished to define the importance of the nature of the P1 residue in the autocatalytic processing of pro-PCSK9 into PCSK9 within the ER environment (4, 8). Accordingly, we first undertook a biosynthetic analysis of the WT PCSK9 (Gln$^{152}$) and all its possible P1 (site of autocatalytic cleavage of pro-PCSK9 into PCSK9) mutants except Cys following a 3-h [$^{35}$S]Met/Cys pulse labeling of HEK293 cells transiently expressing these C-terminally V5-tagged constructs. The results of immunoprecipitations with a mAb-V5 followed by SDS-PAGE of cell extracts and media are shown in Fig. 1*A*. It is evident that the P1 residue Gln$^{152}$ is the favored residue because it allowed the most effective autocatalytic processing of pro-PCSK9 into PCSK9 followed by its maximal secretion. The previously reported small amount of the inactive furin-cleaved form at Arg$^{218}$ ↓, namely PCSK9-ΔN$^{218}$ (27), was also present. We also noticed that Gln$^{152}$ could be replaced by Ala, Met, Thr, Ser, or Asn and still allow for some autoprocessing and secretion, albeit at significantly lower levels. All other P1 mutants resulted in the intracellular accumulation of pro-PCSK9, likely in the ER (4, 8, 9). To better evaluate the ratios of secreted PCSK9 *versus* intracellular pro-PCSK9, we performed a similar experiment but quantitated these human proteins in cells and media by an ELISA that recognizes all forms of human PCSK9 (28). The triplicate data obtained are summarized in Fig. 1*B*, and the percent ratios of immunoreactive PCSK9 in the media over cells are shown in Fig. 1*C*. These steady-state results confirm and extend the 3-h pulse labeling data of Fig. 1*A* and allow us to determine a rank order of preference for the P1 residue, namely Gln > Met > Ala > Ser > Asn ≈ Thr ≫ Tyr > Phe. All other P1 residues are essentially not cleaved, including Glu, Asp, Gly, His (a natural mutant (15)), Ile, Lys, Leu, Pro, Arg, Val, and Trp (Fig. 1*C*). It was repeatedly noted that the mutants Q152G, Q152S, and Q152L result in seemingly lower levels of PCSK9 expression within the 3-h pulse. However, this was not seen when the overnight media were analyzed by ELISA (Fig. 1*C*) or Western blotting (Fig. 2*A*). Interestingly, the Q152N mutant and to a lesser extent the Q152T mutant resulted in a PCSK9 that is secreted but much more sensitive to furin inactivation into PCSK9-ΔN$^{218}$ (Fig. 2*A*, *media*), emphasizing the importance of Gln$^{152}$ in protecting the processed WT PCSK9 from excessive cleavage inactivation by furin at the cell surface (29).

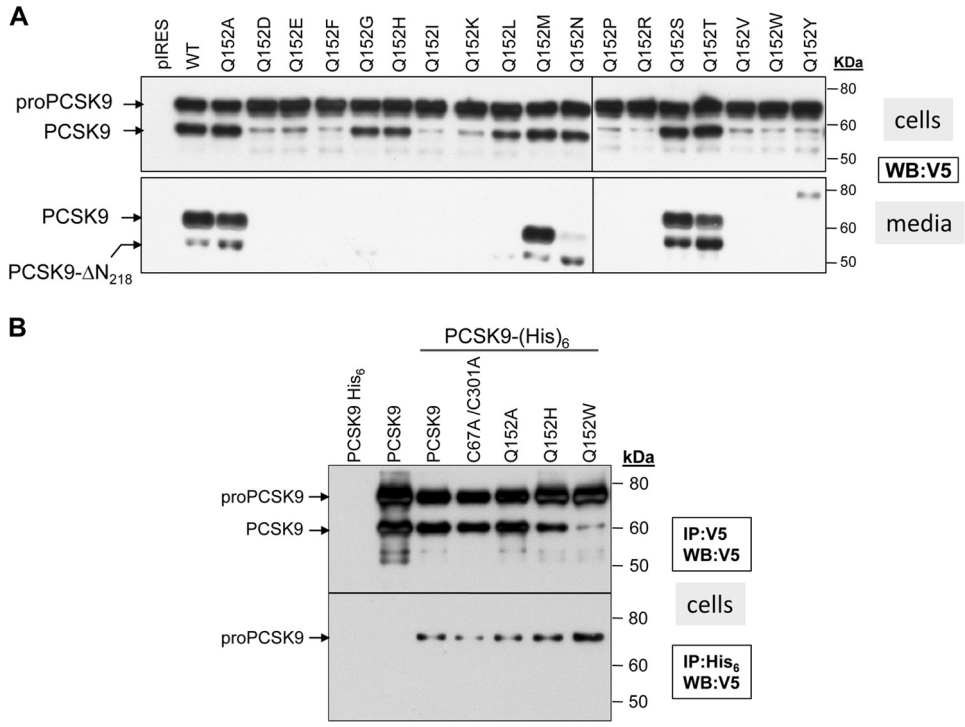


FIGURE 2. **Steady-state expression and secretion of PCSK9 Gln$^{152}$ mutants and their oligomerization.** *A*, 24 h after transfection of HEK293 cells, the expression and secretion of PCSK9 Gln$^{152}$ mutants were analyzed by Western blot (*WB*) using mAb-V5. *B*, HEK293 cells were transfected with V5-tagged PCSK9 and its C67A/C301A, Q152A, Q152H, and Q152W mutants with PCSK9-His$_6$ or without (control). 24 h post-transfection, cell lysates were immunoprecipitated (*IP*) with mAb-V5 or mAb-His$_6$, and the immunoprecipitates were resolved by SDS-PAGE and analyzed by Western blot using mAb-V5-HRP. The migration positions of pro-PCSK9 and PCSK9 as well as that of the furin-cleaved form PCSK9-ΔN$^{218}$ are shown. This figure is representative of at least three independent experiments.

To gain more insights on the longer term effects of the P1 variants, we next undertook a steady-state analysis of the forms of PCSK9 from cells and media. Under Western blot conditions 24 h after transfection, we began to see differences in the intracellularly accumulated forms of some Gln$^{152}$ mutants as compared with the 3-h pulse experiment (compare cells in Figs. 1*A* and 2*A*). Thus, although all mutants exhibited over time a variable extent of intracellular autocatalytic cleavage of pro-PCSK9 into PCSK9, the prominent mutants are Gln, Ala, Gly, His, Leu, Met, Asn, Ser, and Thr. However, only pro-PCSK9 containing a P1 Gln, Ala, Met, Asn, Ser, and Thr allow the secretion of PCSK9. This suggested that even though autocatalytic processing of pro-PCSK9 into PCSK9 in the mutants Q152G, Q152H, and Q152L (underlined above) can partially occur the proteins are not secreted as was also observed for both the LOF C679*X* truncated mutant (27, 30) and E498K (supplemental Fig. S1).

In a remarkable study, Mayne *et al.* (15) showed that the Q152H natural mutation resulted in the accumulation of pro-PCSK9 in the ER (15) as confirmed and refined here (Figs. 1*A* and 2*A*). Interestingly, when this mutant was co-expressed with a WT sequence with Gln$^{152}$, it retained the WT protein intracellularly as pro-PCSK9 and prevented its secretion (15). For a quantitative approach, we co-expressed untagged PCSK9 (native) with the V5-tagged Gln$^{152}$ mutants and analyzed the total levels of PCSK9 in cells and media by our sensitive ELISA (28). The data obtained (supplemental Table S1) revealed that the largest dominant negative effect was observed with the mutants that were not secreted: Q152L, Q152H, Q152F, Q152Y, Q152I, Q152P, Q152R, Q152V, Q152K, Q152E, Q152D, and Q152W (supplemental Table S1). Note also that replacement of Gln$^{152}$ by Met$^{152}$ did not affect the level of secretion of PCSK9, and hence, Met is the only amino acid that is as well tolerated as Gln at the zymogen processing site.

When compared with the ER stress induced upon incubation of cells with the *N*-glycosylation inhibitor tunicamycin, the observed dominant negative effect of the Gln$^{152}$ mutants is not the result of ER stress due to their overexpression in HEK293 cells as evidenced by Xbp-1 amplicons amplified by RT-PCR (25, 31). The data show that only the ER stress inducer tunicamycin enhanced the levels of spliced Xbp-1, resulting in a 263-bp amplicon (26), whereas expression of the PCSK9 constructs did not grossly modify the ratio of the 289-bp unspliced Xbp-1 to the spliced 263-bp form (not shown).

Previously, we reported that following synthesis only the zymogen pro-PCSK9, but not the processed PCSK9, can oligomerize with itself in the ER and that this multimerization requires disulfide bonding (4). In agreement, co-expression of C-terminally His-tagged PCSK9-His$_6$ with V5-tagged PCSK9 revealed that pro-PCSK9-His$_6$ co-immunoprecipitated with the V5-tagged protein in cells (Fig. 2*B*), but no co-immunoprecipitation of PCSK9 was observed in the media (not shown). The same was found for the V5-tagged Q152A, Q152H, and Q152W mutants and the secretable double mutant of WT PCSK9 in which the only two free Cys$^{67}$ and Cys$^{301}$ (11) were mutated to Ala (Fig. 2*B*). We conclude that multimerization of pro-PCSK9 does not depend on Gln$^{152}$ and that the absence of free Cys in pro-PCSK9-C67A/C301A does not prevent its co-immunoprecipitation with WT pro-PCSK9-His$_6$.

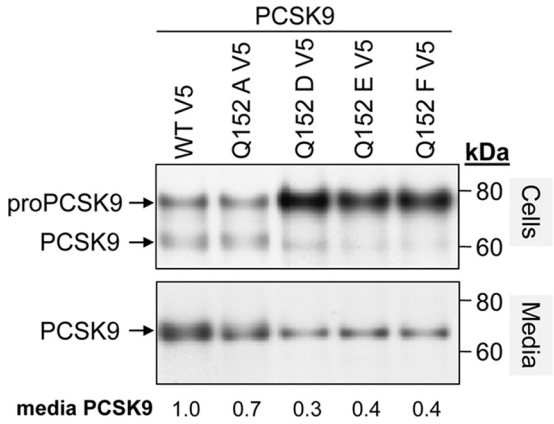


FIGURE 3. **Inhibition of zymogen processing by Gln$^{152}$ mutants.** HEK293 cells were transiently co-transfected with untagged PCSK9 (native PCSK9) and WT PCSK9-V5 or its Q152A, Q152D, Q152E, and Q152F mutants. 48 h post-transfection, the cells were radiolabeled for 3 h with [$^{35}$S]Met/Cys. The media and cell lysates were then immunoprecipitated with a PCSK9-specific antibody (9), the immune complexes were resolved by SDS-PAGE, and the dried gel was autoradiographed. This figure is representative of at least three independent experiments.

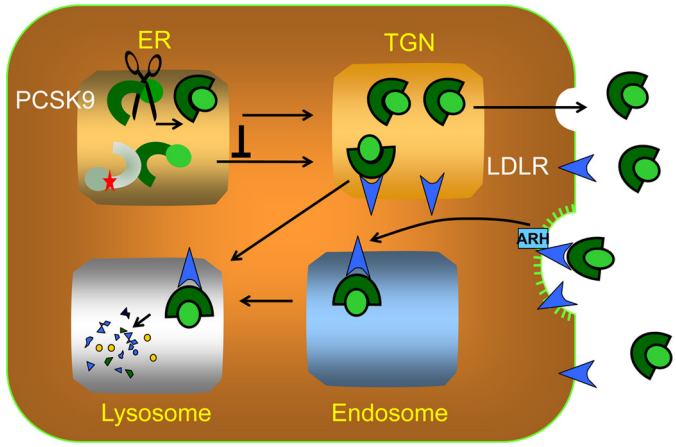


FIGURE 4. **Model of the dominant negative effect of PCSK9 mutants.** In the ER, pro-PCSK9 undergoes an autocatalytic cleavage into PCSK9. The cleaved prosegment (*light green*) associates with the catalytic fragment (*dark green*) and functions as a chaperone, permitting the mature protein to move from the ER into the secretory pathway. Current evidence indicates that PCSK9 might work at two cellular sites. The first potential location is in a post-ER compartment, depicted here as the Golgi apparatus, where PCSK9 might target the LDLRs (*blue*) for degradation in an acidic compartment such as lysosomes. In the second possible pathway, the PCSK9 that is secreted binds to LDLRs on the cell surface. The LDLR·PCSK9 complex is then internalized in clathrin-coated (*green bars*) early endosomes together with the adaptor protein autosomal recessive hypercholesterolemia (*ARH*) (*light blue*). PCSK9 prevents the recycling of the LDLR from the endosome back to the cell surface by directing the LDLR to the lysosome where it is degraded. If pro-PCSK9 cannot be processed (*red star* in a *gray background*; *e.g.* because of a heterozygous natural mutation such as Q152H) it remains as a zymogen in the ER and binds the non-mutated WT zymogen and prevents its processing, thereby acting as a dominant negative, effectively preventing PCSK9 secretion. *TGN*, *trans*-Golgi network.

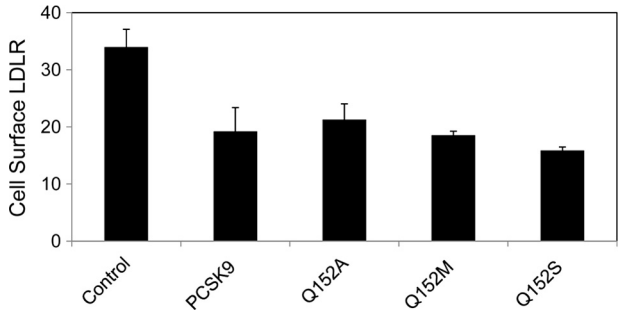


FIGURE 5. **FACS analysis of LDLR following PCSK9 incubations.** HuH7 cells were incubated for 24 h with 750 ng/ml WT PCSK9 or its Q152A, Q152M, and Q152S mutants. The levels of cell surface LDLR were then quantitated by FACS analysis. Although WT PCSK9 and its Q152A, Q152M, and Q152S mutants significantly and similarly reduce cell surface LDLR levels by ~50%, their individual LDLR-reducing activities are not statistically different. This figure is representative of three independent experiments done in triplicate. The *error bars* above the mean value represent the range of values ± standard deviation from the mean.

Biosynthetic analysis of the co-expression of native PCSK9 with the representative V5-tagged Q152A, Q152D, Q152 E, and Q152F mutants is depicted in Fig. 3. The data show that although co-expression of WT PCSK9 with the mutant Q152A did not significantly affect the intracellular zymogen processing the three other non-secretable mutants reduced the levels of the autocatalytic cleavage of pro-PCSK9 into PCSK9 in the cells and substantially increased the relative levels of pro-PCSK9 (Fig. 3).

Thus, it is possible at least in part that the dominant negative effect observed is due to inhibition of the zymogen processing, of WT pro-PCSK9 by mutants that cannot undergo autocatalytic processing and that oligomerize with themselves and/or the WT zymogen. These data suggest that it is likely that most forms of PCSK9 that can barely exit from the ER or not exit at all (*i.e.* remain endoglycosidase H-sensitive; not shown) will more or less efficaciously retain WT pro-PCSK9 within the ER in the cell. A plausible working model is presented in Fig. 4.

We next wished to gauge the activity of the secreted Gln$^{152}$ mutants by their ability to enhance the degradation of the LDLR on the cell surface of HuH7 cells (32). Accordingly, WT PCSK9 and its Q152A, Q152M, and Q152S mutants were produced in HEK293 cells, and their levels in the media were analyzed by ELISA. Equal amounts of these proteins (750 ng/ml) were then incubated at 37 °C for 4 h with HuH7 cells, and then the levels of cell surface LDLR were quantified by FACS. In this assay, the activities of the mutants Q152A, Q152M, and Q152S were similar to that of WT PCSK9 (Fig. 5). These data demonstrated that although the mutants Q152A, Q152M, and Q152S are secreted less than WT PCSK9 (Figs. 1*C* and 2*A*, *media*), when incubated at equal concentrations, their activities on cell surface LDLR are similar to that of WT, and all significantly reduced LDLR levels compared with control (Fig. 5). Thus, the LOF of the Q152A and Q152S mutants would mostly be due to their decreased levels in the media and not to a significant loss of intrinsic activity once secreted.

*Exchangeability of the Prosegment of PCSK9*—The above data suggested that inhibition of the zymogen processing of PCSK9 may be a novel approach to block the secretion of PCSK9 and hence its activity on the LDLR. Co-expression of the WT protein with a mutant that cannot undergo zymogen processing is one way to achieve this goal. Another approach would be to inhibit the catalytic site of pro-PCSK9 and prevent its zymogen processing. This method was used previously to inhibit the convertases furin, PC7 (33), and PC5/6 (34) via the expression of the inhibitory WT prosegment in *trans*.

Herein, we investigated the effect of overexpression of the N-terminally V5-tagged WT prosegment on the secretion of native PCSK9. Biosynthetic analysis revealed that a small per-

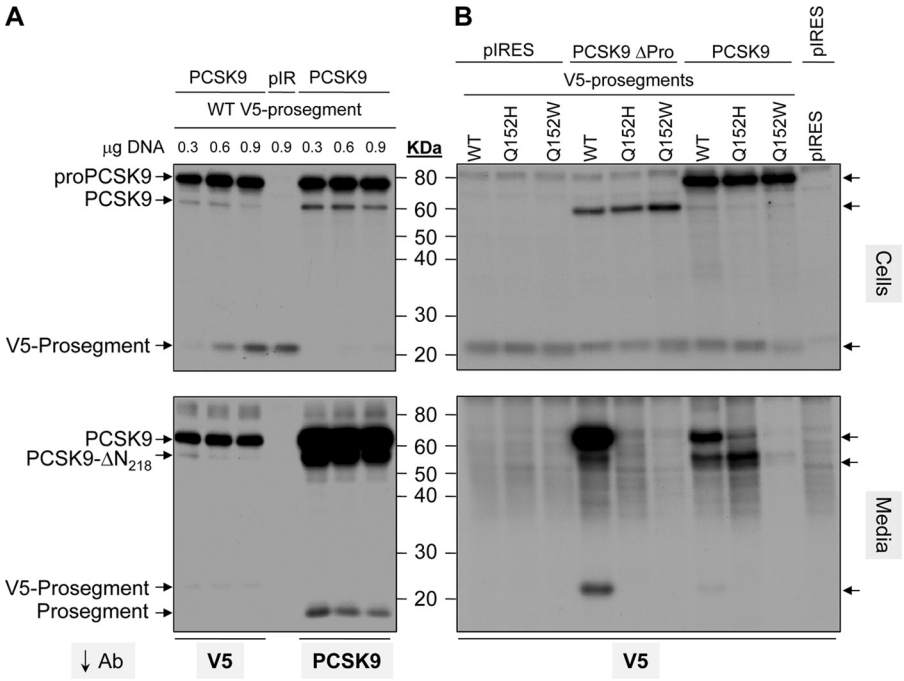


FIGURE 6. **Exchangeability of the prosegment of PCSK9.** *A*, HEK293 cells were transiently co-transfected with 0.5 $\mu$g of untagged PCSK9 (native PCSK9) and increasing amounts (0.3, 0.6, and 0.9 $\mu$g) of a cDNA coding for the WT V5-prosegment of PCSK9. 48 h post-transfection, the cells were radiolabeled for 4 h with [$^{35}$S]Met/Cys. The media and cell lysates were then immunoprecipitated with mAb-V5 or a PCSK9-specific antibody, and the immune complexes were resolved by SDS-PAGE. *B*, HEK293 cells were transiently co-transfected with 0.5 $\mu$g of pIRES vector, untagged PCSK9-Δpro (native PCSK9-Δpro), or native PCSK9 together with 0.5 $\mu$g of a cDNA coding for the WT V5-prosegment of PCSK9 or its Q152H and Q152W mutants. 48 h post-transfection, the cells were radiolabeled for 4 h with [$^{35}$S]Met/Cys. The media and cell lysates were then immunoprecipitated with mAb-V5, and the immune complexes were resolved by SDS-PAGE. The migration positions of pro-PCSK9 and PCSK9 as well as that of the furin-cleaved form, PCSK9-ΔN$^{218}$, and those of the V5- and untagged prosegments are emphasized. The control consisted of replacing the native PCSK9 by the empty vector pIRES (*pIR*). This figure is representative of two independent experiments. *Ab*, antibody.

centage of intracellular untagged pro-PCSK9 and secreted PCSK9 co-immunoprecipitated with the V5-tagged prosegment (Fig. 6*A*). By using a PCSK9-specific antibody (9), we estimated that this represents <10%, suggesting that the WT prosegment in *trans* can replace, albeit not efficiently, that of pro-PCSK9. These data demonstrated that the V5-prosegment can bind pro-PCSK9 before the occurrence of zymogen processing in the ER and that it can also partially replace the WT sequence of the processed and secreted PCSK9 (Fig. 6*A*, *media*). A similar low exchange efficiency has already been seen upon expression of the WT prosegment of the convertase SKI-1/S1P with the full-length enzyme, leading us to engineer a prosegment with a specific point mutation (R134E) at the autocatalytic B/B′ site that enhanced its inhibitory effect on SKI-1/S1P (35).

We showed previously that co-expression of WT native PCSK9 lacking the prosegment (native PCSK9-Δpro) with an N-terminally V5-tagged prosegment allows the secretion of native PCSK9 in complex with the V5-tagged prosegment (14). Upon co-expression of native PCSK9-Δpro with V5-tagged prosegment mutants ending with His$^{152}$ or Trp$^{152}$ instead of the WT Gln$^{152}$, we noted that although all prosegments co-immunoprecipitated with native PCSK9-Δpro in cells (likely in the ER) the only V5-prosegment·native PCSK9 complex secreted was that carrying the WT Gln$^{152}$ (Fig. 6*B*). Furthermore, co-expression of the full-length native PCSK9 with the same prosegments also revealed that, like the WT, the mutant prosegments bound the zymogen pro-PCSK9 in the cell. Here again, the WT V5-prosegment allowed secretion of the mature V5-prosegment·PCSK9 complex. Interestingly, the prosegment ending with the natural mutation Q152H resulted in a complex that is readily cleaved by furin into native PCSK9-ΔN$^{218}$, whereas the prosegment ending with Trp$^{152}$ did not allow any secretion of native PCSK9 bound to the V5-prosegment (Fig. 6*B*). However, the use of a PCSK9 antibody instead of mAb-V5 revealed that here again ≪10% of the total secreted native PCSK9 originating from pro-PCSK9 is bound to the V5-prosegment (see supplemental Fig. S2, arrow ). Finally, the latter data show that overexpression of the WT or mutant prosegments with pro-PCSK9 did not result in inhibition of intracellular zymogen processing or in a significant reduction in the level of secreted WT PCSK9 (supplemental Fig. S2). We conclude that, contrary to other convertases (33–35), in *trans* overexpression of the prosegment or its Gln$^{152}$ mutants does not inhibit PCSK9 processing or secretion; however, only a negligible amount of prosegment can be replaced in pro-PCSK9.

*The Dominant Negative Effects of Multiple PCSK9 Mutants*—We next tackled the question of whether the dominant negative effect observed with the Gln$^{152}$ mutants would also be seen with other selected natural and/or artificial PCSK9 variants that occur in the prosegment (amino acids 31–152) as well as in the catalytic and CHRD domains (amino acids 153–692). Herein, we concentrated on mutants that significantly reduce or abolish the secretion of PCSK9 (8).

Analysis of the media and cell extracts by ELISA of the V5-tagged PCSK9 lacking its prosegment (Δpro) (14, 32) and

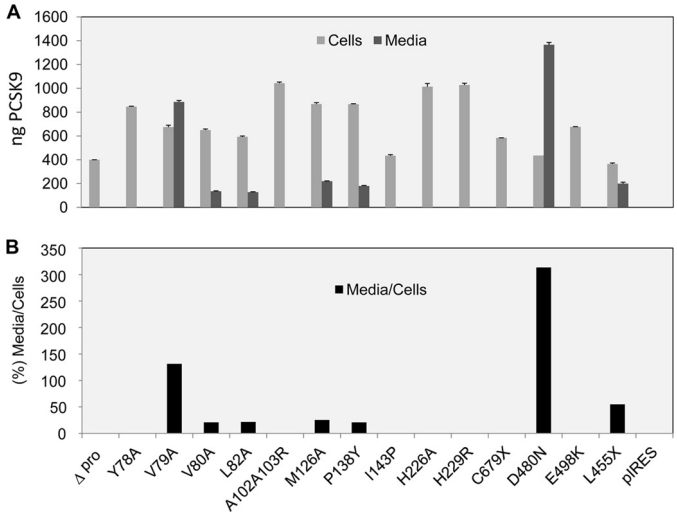


FIGURE 7. **Expression and secretion of PCSK9 mutants.** HEK293 cells were transiently transfected with 0.5 $\mu$g of PCSK9-V5 mutants in the prosegment (Y78A, V79A, V80A, L82A, A102A103R, M126A, P138Y, and I143P), catalytic domain (active site mutant H226A and H229R), or CHRD (C679*X*, D480N, E498K, and L455*X*) or with an empty vector control pIRES. *A*, 24 h post-transfection, cells were washed and incubated for another 24 h in RPMI 1640 medium + 5% lipoprotein-deficient serum. PCSK9 in the media and cell lysates was then quantitated by ELISA. *B*, calculated percent ratio of PCSK9 in media/cells. This figure is representative of three independent experiments done in triplicate. The *error bars* above the mean value represent the range of values ± standard deviation from the mean.

those of the PCSK9 prosegment mutants Y78A, V79A, V80A, L82A, A102,103R, M126A, P138Y, and I143P is shown in Fig. 7. The data revealed that the V79A variant is about half as well secreted as WT PCSK9 (compare Figs. 1*C* and 7*B*) and that all other prosegment mutants selected are not secreted. Within the catalytic subunit, we selected the active site His* mutant H226A (4) as well as the nearby artificial mutant H229R. This new mutation was chosen because the site equivalent to $His^{229}$ in PCSK9 is highly conserved between species and invariably occupied by an Arg residue in all eight other members of the proprotein convertase family (36). The other variants selected included the natural LOF mutant C679*X* (37), the recently described natural Mexican mutations D480N and E498K (38), and PCSK9-L455*X* (lacking the C-terminal CHRD domain amino acids 455–692) that is secreted but inactive (32). The data show that the D480N mutant was as well secreted as the WT (compare Figs. 1*C* and 7*B*) and that the L455*X* mutant was ~7-fold less secreted from HEK293 cells than the WT as reported (32). All other catalytic domain mutants chosen were not secreted.

We next co-expressed equal amounts of cDNAs coding for native PCSK9 with the above V5-tagged PCSK9 mutants and analyzed their total levels in cells and media by ELISA. The data obtained (supplemental Table S2) revealed that the largest dominant negative effect was observed with the mutants that are not well secreted or not secreted at all. Those that had the least effect were D480N, L455*X*, and V79A. All other mutants had a significant lowering effect on the secretion of WT PCSK9 (supplemental Table S2).

*The Zymogen Processing of Pro-PCSK9*—The fact that WT pro-PCSK9, but not PCSK9, oligomerizes in the ER (Fig. 2*B*) (4) suggested that it is possible that the dimerization of pro-PCSK9 may cause an exchange of prosegment between the monomers and that such an exchange may be occurring during autocatalytic processing. To test this hypothesis, we transiently expressed WT PCSK9 tagged at the N terminus of its prosegment with V5 or at the C terminus of the whole protein with a red fluorescent protein (RFP of ~20 kDa) individually or both together for 24 h in HEK293 cells. The addition of the RFP domain to the C terminus of PCSK9 did not affect the autoprocessing of pro-PCSK9-RFP, the secretion of PCSK9-RFP, or its activity on the LDLR (not shown). The cell lysates and media were immunoprecipitated with mAb-V5, an RFP-specific antibody, or our PCSK9 antibody (9). The precipitates were then resolved by SDS-PAGE, and the separated proteins were analyzed by Western blot using one of the above three antibodies (supplemental Fig. S3). The data clearly show that the cross-complex V5-prosegment·PCSK9-RFP is never detected in the media or cells because immunoprecipitation with mAb-V5 never leads to co-immunoprecipitation of PCSK9-RFP and vice versa. We conclude that zymogen processing of pro-PCSK9 into PCSK9 is intramolecular for each monomer as is the case for all other mammalian PC family members (1) and related bacterial subtilases (39).

*The Effect of Various $Tyr^{374}$ Mutations on the Activity of PCSK9 on the LDLR*—The Anglo-Saxon mutation in which the $Asp^{374}$ is replaced by a Tyr (D374Y) resulted in 10–25-fold enhanced binding of PCSK9 to the EGF-A domain of the LDLR (11, 20, 40). A similarly increased LDLR degradation activity by PCSK9 was also reported for the Portuguese GOF D374H natural mutation (23). We therefore investigated whether residues other than $Tyr^{374}$ or $His^{374}$ could also result in a similar GOF. Accordingly, $Asp^{374}$ was replaced by all amino acids except Cys, and the biosynthesis and secretion of all such mutants were analyzed following a 3-h pulse with [$^{35}$S]Met/Cys. The data show that all mutants were well processed and secreted except for D374P, which seemed to be cleaved to a much lower molecular mass form that remained in the cell (Fig. 8). We also noted a slight rise in the apparent molecular mass of the D374N possibly due to *N*-glycosylation at the resulting consensus $\underline{Asn}^{374}$-Cys-$\underline{Ser}$ site (where the underlined residues are the critical recognition motif for N-glycosylation). These data were confirmed by ELISA analysis of the levels of PCSK9 in the cells and media of these mutants expressed in HEK293 cells (Fig. 9, *A* and *B*). Note that for the non-secretable D374P mutant the cellular levels were low (Fig. 9*A*), suggesting that the unusually processed form of its zymogen is degraded over time as it now exhibits a Pro-$Cys^{375}$-Ser-Thr-$Cys^{378}$ sequence that may not favor the proper disulfide bond formation of $Cys^{375}$ to $Cys^{378}$ (11).

We next incubated HuH7 cells for 4 h with each of these mutants (all at 800 ng/ml) obtained from HEK293 media (Fig. 9*B*), and the cell surface levels of LDLR were quantified by FACS (32). The data show that except for D374N and less so for D374G (D374P is not secreted), the majority of the other mutants behave as GOF variants with the activity of D374E similar to that of the WT form (Fig. 9*C*). This suggests that replacement of Asp by Glu does not confer any advantage to the PCSK9 activity on the LDLR in our cell-based assay. Thus, it is plausible that the GOF afforded by most other mutants of

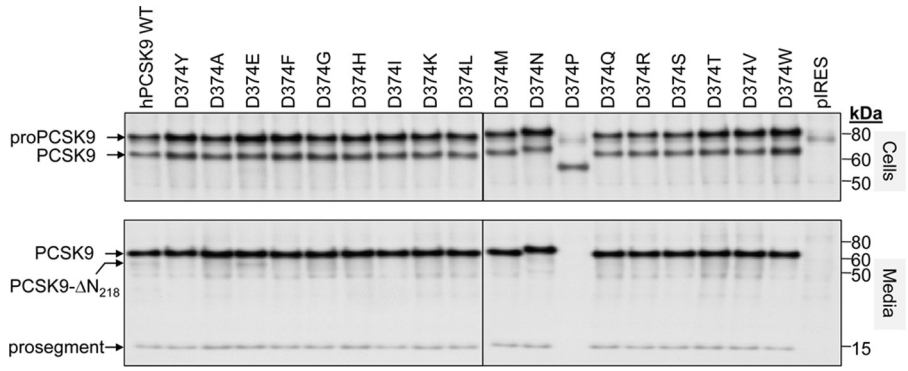


FIGURE 8. **Expression and secretion of PCSK9 Asp$^{374}$ mutants.** HEK293 cells were transiently transfected with WT PCSK9-V5 and its Asp$^{374}$ mutants. 48 h post-transfection, the cells were radiolabeled for 3 h with [$^{35}$S]Met/Cys. The media and cell lysates were then immunoprecipitated with mAb-V5, the immune complexes were resolved by SDS-PAGE on an 8% polyacrylamide Tricine gel, and the dried gel was autoradiographed. The migration positions of pro-PCSK9 and PCSK9 as well as that of the furin-cleaved form, PCSK9-ΔN$^{218}$, and the prosegment are shown. This figure is representative of three independent experiments.

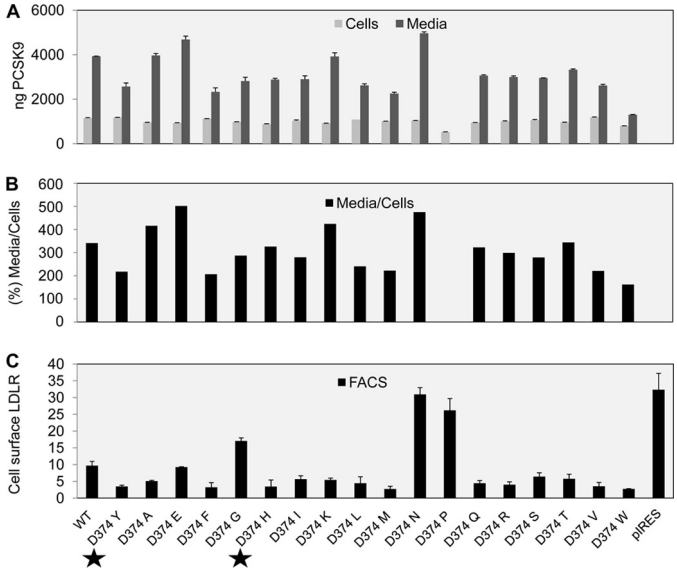


FIGURE 9. **Expression, secretion, and activity of PCSK9 Asp$^{374}$ mutants.** HEK293 cells were transiently transfected with WT PCSK9-V5 and its Asp$^{374}$ mutants. 24 h post-transfection, cells were washed and incubated for another 24 h in RPMI 1640 medium + 5% lipoprotein-deficient serum. *A*, PCSK9 in the media and cell lysates was then quantitated by ELISA. *B*, calculated percent ratio of PCSK9 in media/cells. *C*, HuH7 cells were incubated for 4 h with 800 ng/ml WT PCSK9, its Asp$^{374}$ mutants, or a control vector (pIRES). The levels of cell surface LDLR were then quantitated by FACS analysis. The *stars* point to the two known natural mutants, D374Y and D374H. This figure is representative of three independent experiments done in triplicate. The *error bars* above the mean value represent the range of values ± standard deviation from the mean.

Asp$^{374}$ is due to the loss of the negative charge at amino acid 374.

## DISCUSSION

The discovery of PCSK9 and its critical role in the regulation of the hepatic LDLR (for comprehensive reviews, see Refs. 2 and 41–43) led to novel therapies to reduce the levels of circulating LDL cholesterol. The most successful therapy so far involved the injection of an inhibitory monoclonal antibody that blocks the PCSK9·LDLR interaction both in model mice and human (2, 16, 44). Indeed, Phase II and III clinical trials are ongoing using such an approach combined or not with statin, a widely prescribed orally active cholesterol-lowering drug. However, other approaches using injectable drugs are also being tested, including the use of adnectins and antisense oligonucleotides (2). Recently, a 66-amino acid variant of the LDLR′ EGF-A peptide fused to immunoglobulin Fc (EGF66-Fc) was reported to be potentially useful to compete with the LDLR for PCSK9 (45). Finally, we showed that a synthetic peptide mimicking the R1 domain of Annexin A2 inhibits the PCSK9 activity on LDLR by binding to the C-terminal PCSK9′ CHRD domain and that *in vivo* this mostly occurs in extrahepatic tissues (46, 47). The above studies provided validation of PCSK9 as a viable drug candidate and a proof of principle of the therapeutic benefit of its inhibition. However, in the long run, it is likely that an orally active PCSK9 inhibitor may be more widely usable than injectable biologics for the treatment of hypercholesterolemia.

Among the proposed approaches for orally active compounds is the targeting of the PCSK9·EGF-A interaction using small molecule inhibitors. In part due to the relatively large flat surface of interaction (17, 18), no potent small molecule has yet been reported. Another approach would entail the disruption of the secreted prosegment·PCSK9 complex. However, this complex is very tight as it involves multiple binding sites (11) and is thus conceivably difficult to disrupt. However, it was reported that oxygen exchange can occur in this complex at the catalytic prosegment·PCSK9 binding interface (48), suggesting some flexibility that could be exploited.

Inspired from work on the other proprotein convertases (33, 35), we have thus tried to probe whether overexpression of the prosegment in *trans* could inhibit the autocatalytic processing of pro-PCSK9. The data show that <10% of the V5-tagged prosegment or its Q152H and Q152W mutants expressed in *trans* could substitute for the endogenous prosegment of pro-PCSK9 and that such an approach would not lead to any significant inhibition of zymogen processing or PCSK9 secretion (Fig. 6 and supplemental Fig. S2).

It was first reported by Cariou *et al.* (49) that the PCSK9 natural single allele double mutant R104C/V114A exhibits a drastically reduced autocatalytic processing of pro-PCSK9 and loss of PCSK9 secretion. This heterozygous LOF variant results in undetectable levels of circulating PCSK9. This was rationalized by the dominant negative activity of the R104C/V114A mutant over the WT allele that is associated with an increased

LDL cholesterol catabolic rate in human (49). In a similar vein, Mayne *et al.* (15) showed that the heterozygous natural mutation Q152H at the autocatalytic cleavage site $Gln^{152}$ results in much reduced circulating levels of PCSK9 and that pro-PCSK9-Q152H is not processed and acts as a dominant negative on the WT allele. The identification of two LOF mutations in the prosegment (R104C/V114A and Q152H) that resulted in a dominant negative phenotype prompted us to evaluate a large number of reported natural and artificial mutants that also exhibit processing and/or secretion defects. Indeed, all the mutants we analyzed also showed a correlation between the extent of loss of zymogen processing/secretion and their ability to act as dominant negatives in inhibiting the zymogen processing and/or secretion of PCSK9 (supplemental Tables S1 and S2 and Figs. 4 and 5).

The mechanism behind the observed dominant negative property of missense PCSK9 mutations that result in loss of secretion is likely related to the property of pro-PCSK9 to oligomerize in the ER (4) as also evidenced by the co-immunoprecipitation of co-expressed zymogens (Fig. 2*B*). Our results showed that the Q152D, Q152E, and Q152F mutants that exhibit loss of zymogen processing can also inhibit the zymogen processing of the co-expressed WT form (Fig. 3). However, so far we have not been able to identify a motif or sequence that would regulate the disulfide bond-dependent oligomerization propensity of pro-PCSK9. Indeed, all the deletion mutants of PCSK9 analyzed oligomerize, including the prosegment alone, PCSK9-Δpro, PCSK9-L455*X* lacking the C-terminal CHRD, and the various missense mutants presented in this work (not shown). This was evidenced by SDS-PAGE analysis in the absence of β-mercaptoethanol, which showed a number of higher molecular mass oligomers and the absence of monomers as reported earlier (4). The only exception is the CHRD domain itself, which when expressed as a secretory protein (9, 46) does not oligomerize (not shown).

Because PCSK9 is tightly bound to its inhibitory prosegment (4) and never seems to detach from it (8, 11), it was not surprising that its ability to enhance the degradation of LDLR (12, 13), VLDL receptor, and ApoER2 (14) is not dependent on its catalytic activity. Accordingly, the only known substrate of PCSK9 is itself, and its catalytic activity is required for the zymogen processing of pro-PCSK9 into PCSK9 (4). Early attempts to use mutagenesis of the autocatalytic cleavage site $VFAQ^{152}\downarrow$ to define the specificity of PCSK9 revealed that the P1 Gln can be replaced by Ala and that the aliphatic Val at P4 is critical (8). In this report, analysis of the P1 $Gln^{152}$ autocleavage specificity revealed a rank order of preference for the P1 position of Gln > Met > Ala > Ser > Thr ≈ Asn. All other residues led to the formation of an unprocessed zymogen that acted as a dominant negative retaining the WT zymogen in the cell (Figs. 3 and 4 and supplemental Table S1). The loss of zymogen processing of these P1 mutants does not seem to be primarily due to the inability of their prosegment to bind to PCSK9 (Fig. 6). This suggests that the major stumbling block abrogating zymogen processing in these mutants may be related to catalytic peptide bond cleavage efficacy rather than active site binding of these $Gln^{152}$ mutants.

It was observed that some PCSK9 mutants can undergo autocatalytic cleavage in the ER but are not secreted (8, 27, 37). Normally, once cleaved in the ER, the prosegment remains tightly bound to PCSK9 and is secreted as a prosegment·PCSK9 complex (4). Some of the processed PCSK9 mutants lose their tight grip on their prosegments, *e.g.* E498K and C672X (supplemental Fig. S1), which may explain why they are not secreted.

We next turned our attention to the less prevalent GOF natural mutations of PCSK9 associated with autosomal dominant hypercholesterolemia (5). Only a few GOF mutations have been reported in autosomal dominant hypercholesterolemia (ADH) (for a review, see Ref. 50). Their identification was crucial in studying the role of PCSK9 in hypercholesterolemia and its impact on the LDLR. Recently, we identified a novel prosegment L108R natural GOF mutant that enhances the interaction of the prosegment of PCSK9 with the β-barrel domain of the LDLR (51). Nevertheless, the most damaging mutation is the Anglo-Saxon-associated D374Y mutation (19) that increases by 10–25-fold the affinity of PCSK9 for the LDLR (11), enhances LDLR degradation (21), and increases apolipoprotein B secretion (52). The reported co-crystal structure of PCSK9 with the EGF-A domain of the LDLR (17) revealed that at acidic pH values $Asp^{374}$ in PCSK9 forms a critical hydrogen bond with $His^{327}$ within the EGF-A domain. Based on binding studies and co-crystal structure analysis, this hydrogen bond was shown to be strengthened at neutral pH for the H327Y mutant of the LDLR (53). It was therefore of interest to investigate whether $Asp^{374}$ variants of PCSK9 might maintain, abolish, or enhance the activity of PCSK9 on LDLR. Previously, the GOF natural mutant D374H has been reported in Portuguese family members suffering from familial hypercholesterolemia (23). Furthermore, a limited vertical scanning mutagenesis study of $Asp^{374}$ revealed the following rank order of binding affinities to immobilized soluble LDLR: Tyr ≈ Phe ≫ Leu ≈ Ala > Lys ≈ Glu ≈ $Asp^{374}$ (40).

In the present study, we systematically mutagenized $Asp^{374}$ to all possible residues except Cys and analyzed their zymogen processing and secretion (Fig. 8) as well as their activity by FACS analysis of cell surface LDLR of HuH7 cells incubated for 4 h at 37 °C with an 800 ng/ml concentration of each mutant protein (Fig. 9). Although most PCSK9 mutants exhibited a stronger ability to lower the levels of cell surface LDLR as compared with WT $Asp^{374}$ (Fig. 9*C*), we noted that D374N is inactive and D374G is less active than WT PCSK9. Although well secreted (Figs. 8 and 9*B*), the D374N mutant is probably *N*-glycosylated at the newly created consensus $Asn^{374}$-Cys-Ser motif (Fig. 8), likely affecting its conformation and resulting in a LOF. The D374G is well processed and secreted (Figs. 8 and 9*B*) but probably does not adopt a favorable conformation for activity on LDLR. The D374P is not secreted at all and seems to be degraded intracellularly (Fig. 8). It is to be noted that our cellular incubation results revealed that WT and D374E PCSK9 have very similar activities toward the cell surface LDLR (Fig. 9), similar to what was reported based on FRET-based binding data (40). However, different from the latter study, we did not see a large difference between the activities of the D374K and D374L mutants. This may be attributable to using HuH7 cells here as opposed to *in vitro* binding to soluble LDLR in the earlier study

(40). Nevertheless, we can conclude that replacement of the negatively charged $Asp^{374}$ by another acidic residue (D374E) does not influence its activity at neutral pH but that most other mutations that result in a secretable protein exhibit considerable GOF activities with $Trp^{374}$, $Met^{374}$, $His^{374}$, $Phe^{374}$, and $Tyr^{374}$ being the most potent PCSK9 variants.

In conclusion, the results presented in this work reveal the critical importance of the P1 $Gln^{152}$ for efficient autocatalytic processing of pro-PCSK9 and demonstrate that PCSK9 has limited enzymatic cleavage specificity on itself as a substrate. The unexpected general observation that PCSK9 mutants that cannot undergo zymogen processing or productive folding result in a dominant negative form of the protein has fundamental clinical implications. The search for small molecules that would disrupt the zymogen processing and/or folding of the processed PCSK9 represents a novel approach to inhibit the activity of PCSK9 with the aim of reducing LDL cholesterol.

*Acknowledgments—We are grateful to Dr. Maryssa Canuel for help with the generation of the cDNA construct PCSK9-RFP and to Marie-Claude Asselin for excellent technical assistance. We thank Brigitte Mary for efficacious editorial assistance.*

## REFERENCES


1. Seidah, N. G., Mayer, G., Zaid, A., Rousselet, E., Nassoury, N., Poirier, S., Essalmani, R., and Prat, A. (2008) The activation and physiological functions of the proprotein convertases. *Int. J. Biochem. Cell Biol.* **40,** 1111–1125
2. Seidah, N. G., and Prat, A. (2012) The biology and therapeutic targeting of the proprotein convertases. *Nat. Rev. Drug Discov.* **11,** 367–383
3. Chrétien, M. (2012) My road to Damascus: how I converted to the prohormone theory and the proprotein convertases. *Biochem. Cell Biol.*, in press
4. Seidah, N. G., Benjannet, S., Wickham, L., Marcinkiewicz, J., Jasmin, S. B., Stifani, S., Basak, A., Prat, A., and Chretien, M. (2003) The secretory proprotein convertase neural apoptosis-regulated convertase 1 (NARC-1): liver regeneration and neuronal differentiation. *Proc. Natl. Acad. Sci. U.S.A.* **100,** 928–933
5. Abifadel, M., Varret, M., Rabès, J. P., Allard, D., Ouguerram, K., Devillers, M., Cruaud, C., Benjannet, S., Wickham, L., Erlich, D., Derré, A., Villéger, L., Farnier, M., Beucler, I., Bruckert, E., Chambaz, J., Chanu, B., Lecerf, J. M., Luc, G., Moulin, P., Weissenbach, J., Prat, A., Krempf, M., Junien, C., Seidah, N. G., and Boileau, C. (2003) Mutations in PCSK9 cause autosomal dominant hypercholesterolemia. *Nat. Genet.* **34,** 154–156
6. Maxwell, K. N., and Breslow, J. L. (2004) Adenoviral-mediated expression of Pcsk9 in mice results in a low-density lipoprotein receptor knockout phenotype. *Proc. Natl. Acad. Sci. U.S.A.* **101,** 7100–7105
7. Maxwell, K. N., Fisher, E. A., and Breslow, J. L. (2005) Overexpression of PCSK9 accelerates the degradation of the LDLR in a post-endoplasmic reticulum compartment. *Proc. Natl. Acad. Sci. U.S.A.* **102,** 2069–2074
8. Benjannet, S., Rhainds, D., Essalmani, R., Mayne, J., Wickham, L., Jin, W., Asselin, M. C., Hamelin, J., Varret, M., Allard, D., Trillard, M., Abifadel, M., Tebon, A., Attie, A. D., Rader, D. J., Boileau, C., Brissette, L., Chrétien, M., Prat, A., and Seidah, N. G. (2004) NARC-1/PCSK9 and its natural mutants: zymogen cleavage and effects on the low density lipoprotein (LDL) receptor and LDL cholesterol. *J. Biol. Chem.* **279,** 48865–48875
9. Nassoury, N., Blasiole, D. A., Tebon Oler, A., Benjannet, S., Hamelin, J., Poupon, V., McPherson, P. S., Attie, A. D., Prat, A., and Seidah, N. G. (2007) The cellular trafficking of the secretory proprotein convertase PCSK9 and its dependence on the LDLR. *Traffic* **8,** 718–732
10. Naureckiene, S., Ma, L., Sreekumar, K., Purandare, U., Lo, C. F., Huang, Y., Chiang, L. W., Grenier, J. M., Ozenberger, B. A., Jacobsen, J. S., Kennedy, J. D., DiStefano, P. S., Wood, A., and Bingham, B. (2003) Functional characterization of Narc 1, a novel proteinase related to proteinase K. *Arch. Biochem. Biophys.* **420,** 55–67
11. Cunningham, D., Danley, D. E., Geoghegan, K. F., Griffor, M. C., Hawkins, J. L., Subashi, T. A., Varghese, A. H., Ammirati, M. J., Culp, J. S., Hoth, L. R., Mansour, M. N., McGrath, K. M., Seddon, A. P., Shenolikar, S., Stutzman-Engwall, K. J., Warren, L. C., Xia, D., and Qiu, X. (2007) Structural and biophysical studies of PCSK9 and its mutants linked to familial hypercholesterolemia. *Nat. Struct. Mol. Biol.* **14,** 413–419
12. McNutt, M. C., Lagace, T. A., and Horton, J. D. (2007) Catalytic activity is not required for secreted PCSK9 to reduce low density lipoprotein receptors in HepG2 cells. *J. Biol. Chem.* **282,** 20799–20803
13. Li, J., Tumanut, C., Gavigan, J. A., Huang, W. J., Hampton, E. N., Tumanut, R., Suen, K. F., Trauger, J. W., Spraggon, G., Lesley, S. A., Liau, G., Yowe, D., and Harris, J. L. (2007) Secreted PCSK9 promotes LDL receptor degradation independently of proteolytic activity. *Biochem. J.* **406,** 203–207
14. Poirier, S., Mayer, G., Benjannet, S., Bergeron, E., Marcinkiewicz, J., Nassoury, N., Mayer, H., Nimpf, J., Prat, A., and Seidah, N. G. (2008) The proprotein convertase PCSK9 induces the degradation of low density lipoprotein receptor (LDLR) and its closest family members VLDLR and ApoER2. *J. Biol. Chem.* **283,** 2363–2372
15. Mayne, J., Dewpura, T., Raymond, A., Bernier, L., Cousins, M., Ooi, T. C., Davignon, J., Seidah, N. G., Mbikay, M., and Chrétien, M. (2011) Novel loss-of-function PCSK9 variant is associated with low plasma LDL cholesterol in a French-Canadian family and with impaired processing and secretion in cell culture. *Clin. Chem.* **57,** 1415–1423
16. Stein, E. A., Mellis, S., Yancopoulos, G. D., Stahl, N., Logan, D., Smith, W. B., Lisbon, E., Gutierrez, M., Webb, C., Wu, R., Du, Y., Kranz, T., Gasparino, E., and Swergold, G. D. (2012) Effect of a monoclonal antibody to PCSK9 on LDL cholesterol. *N. Engl. J. Med.* **366,** 1108–1118
17. Kwon, H. J., Lagace, T. A., McNutt, M. C., Horton, J. D., and Deisenhofer, J. (2008) Molecular basis for LDL receptor recognition by PCSK9. *Proc. Natl. Acad. Sci. U.S.A.* **105,** 1820–1825
18. Surdo, P. L., Bottomley, M. J., Calzetta, A., Settembre, E. C., Cirillo, A., Pandit, S., Ni, Y. G., Hubbard, B., Sitlani, A., and Carfí, A. (2011) Mechanistic implications for LDL receptor degradation from the PCSK9/LDLR structure at neutral pH. *EMBO Rep.* **12,** 1300–1305
19. Timms, K. M., Wagner, S., Samuels, M. E., Forbey, K., Goldfine, H., Jammulapati, S., Skolnick, M. H., Hopkins, P. N., Hunt, S. C., and Shattuck, D. M. (2004) A mutation in PCSK9 causing autosomal-dominant hypercholesterolemia in a Utah pedigree. *Hum. Genet.* **114,** 349–353
20. Fisher, T. S., Lo Surdo, P., Pandit, S., Mattu, M., Santoro, J. C., Wisniewski, D., Cummings, R. T., Calzetta, A., Cubbon, R. M., Fischer, P. A., Tarachandani, A., De Francesco, R., Wright, S. D., Sparrow, C. P., Carfi, A., and Sitlani, A. (2007) PCSK9-dependent LDL receptor regulation: effects of pH and LDL. *J. Biol. Chem.* **282,** 20502–20512
21. Lagace, T. A., Curtis, D. E., Garuti, R., McNutt, M. C., Park, S. W., Prather, H. B., Anderson, N. N., Ho, Y. K., Hammer, R. E., and Horton, J. D. (2006) Secreted PCSK9 decreases the number of LDL receptors in hepatocytes and in livers of parabiotic mice. *J. Clin. Investig.* **116,** 2995–3005
22. Fasano, T., Sun, X. M., Patel, D. D., and Soutar, A. K. (2009) Degradation of LDLR protein mediated by 'gain of function' PCSK9 mutants in normal and ARH cells. *Atherosclerosis* **203,** 166–171
23. Bourbon, M., Alves, A. C., Medeiros, A. M., Silva, S., and Soutar, A. K. (2008) Familial hypercholesterolaemia in Portugal. *Atherosclerosis* **196,** 633–642
24. Benjannet, S., Elagoz, A., Wickham, L., Mamarbachi, M., Munzer, J. S., Basak, A., Lazure, C., Cromlish, J. A., Sisodia, S., Checler, F., Chrétien, M., and Seidah, N. G. (2001) Post-translational processing of $\beta$-secretase ($\beta$-amyloid-converting enzyme) and its ectodomain shedding. The pro- and transmembrane/cytosolic domains affect its cellular activity and amyloid-$\beta$ production. *J. Biol. Chem.* **276,** 10879–10887
25. Lin, J. H., Li, H., Yasumura, D., Cohen, H. R., Zhang, C., Panning, B., Shokat, K. M., Lavail, M. M., and Walter, P. (2007) IRE1 signaling affects cell fate during the unfolded protein response. *Science* **318,** 944–949
26. Yoshida, H., Matsui, T., Yamamoto, A., Okada, T., and Mori, K. (2001) XBP1 mRNA is induced by ATF6 and spliced by IRE1 in response to ER stress to produce a highly active transcription factor. *Cell* **107,** 881–891
27. Benjannet, S., Rhainds, D., Hamelin, J., Nassoury, N., and Seidah, N. G.

(2006) The proprotein convertase PCSK9 is inactivated by furin and/or PC5/6A: functional consequences of natural mutations and post-translational modifications. *J. Biol. Chem.* **281,** 30561–30572
28. Dubuc, G., Tremblay, M., Paré, G., Jacques, H., Hamelin, J., Benjannet, S., Boulet, L., Genest, J., Bernier, L., Seidah, N. G., and Davignon, J. (2010) A new method for measurement of total plasma PCSK9: clinical applications. *J. Lipid Res.* **51,** 140–149
29. Essalmani, R., Susan-Resiga, D., Chamberland, A., Abifadel, M., Creemers, J. W., Boileau, C., Seidah, N. G., and Prat, A. (2011) *In vivo* evidence that furin from hepatocytes inactivates PCSK9. *J. Biol. Chem.* **286,** 4257–4263
30. Kotowski, I. K., Pertsemlidis, A., Luke, A., Cooper, R. S., Vega, G. L., Cohen, J. C., and Hobbs, H. H. (2006) A spectrum of PCSK9 alleles contributes to plasma levels of low-density lipoprotein cholesterol. *Am. J. Hum. Genet.* **78,** 410–422
31. Rousselet, E., Benjannet, S., Hamelin, J., Canuel, M., and Seidah, N. G. (2011) The proprotein convertase PC7: unique zymogen activation and trafficking pathways. *J. Biol. Chem.* **286,** 2728–2738
32. Benjannet, S., Saavedra, Y. G., Hamelin, J., Asselin, M. C., Essalmani, R., Pasquato, A., Lemaire, P., Duke, G., Miao, B., Duclos, F., Parker, R., Mayer, G., and Seidah, N. G. (2010) Effects of the prosegment and pH on the activity of PCSK9: evidence for additional processing events. *J. Biol. Chem.* **285,** 40965–40978
33. Zhong, M., Munzer, J. S., Basak, A., Benjannet, S., Mowla, S. J., Decroly, E., Chrétien, M., and Seidah, N. G. (1999) The prosegments of furin and PC7 as potent inhibitors of proprotein convertases. *In vitro* and *ex vivo* assessment of their efficacy and selectivity. *J. Biol. Chem.* **274,** 33913–33920
34. Nour, N., Basak, A., Chrétien, M., and Seidah, N. G. (2003) Structure-function analysis of the prosegment of the proprotein convertase PC5A. *J. Biol. Chem.* **278,** 2886–2895
35. Pullikotil, P., Vincent, M., Nichol, S. T., and Seidah, N. G. (2004) Development of protein-based inhibitors of the proprotein of convertase SKI-1/S1P: processing of SREBP-2, ATF6, and a viral glycoprotein. *J. Biol. Chem.* **279,** 17338–17347
36. Siezen, R. J., and Leunissen, J. A. (1997) Subtilases: the superfamily of subtilisin-like serine proteases. *Protein Sci.* **6,** 501–523
37. Cohen, J., Pertsemlidis, A., Kotowski, I. K., Graham, R., Garcia, C. K., and Hobbs, H. H. (2005) Low LDL cholesterol in individuals of African descent resulting from frequent nonsense mutations in PCSK9. *Nat. Genet.* **37,** 161–165
38. Gutiérrez-Cirlos, C., Ordóñez-Sánchez, M. L., Tusié-Luna, M. T., Patterson, B. W., Schonfeld, G., and Aguilar-Salinas, C. A. (2011) Familial hypobetalipoproteinemia in a hospital survey: genetics, metabolism and nonalcoholic fatty liver disease. *Ann. Hepatol.* **10,** 155–164
39. Shinde, U., and Thomas, G. (2011) Insights from bacterial subtilases into the mechanisms of intramolecular chaperone-mediated activation of furin. *Methods Mol. Biol.* **768,** 59–106
40. Pandit, S., Wisniewski, D., Santoro, J. C., Ha, S., Ramakrishnan, V., Cubbon, R. M., Cummings, R. T., Wright, S. D., Sparrow, C. P., Sitlani, A., and Fisher, T. S. (2008) Functional analysis of sites within PCSK9 responsible for hypercholesterolemia. *J. Lipid Res.* **49,** 1333–1343
41. Seidah, N. G. (2009) PCSK9 as a therapeutic target of dyslipidemia. *Expert Opin. Ther. Targets* **13,** 19–28
42. Horton, J. D., Cohen, J. C., and Hobbs, H. H. (2009) PCSK9: a convertase that coordinates LDL catabolism. *J. Lipid Res.* **50,** (suppl.) S172–S177
43. Akram, O. N., Bernier, A., Petrides, F., Wong, G., and Lambert, G. (2010) Beyond LDL cholesterol, a new role for PCSK9. *Arterioscler. Thromb. Vasc. Biol.* **30,** 1279–1281
44. Ni, Y. G., Condra, J. H., Orsatti, L., Shen, X., Di Marco, S., Pandit, S., Bottomley, M. J., Ruggeri, L., Cummings, R. T., Cubbon, R. M., Santoro, J. C., Ehrhardt, A., Lewis, D., Fisher, T. S., Ha, S., Njimoluh, L., Wood, D. D., Hammond, H. A., Wisniewski, D., Volpari, C., Noto, A., Lo Surdo, P., Hubbard, B., Carfí, A., and Sitlani, A. (2010) A proprotein convertase subtilisin-like/kexin type 9 (PCSK9) C-terminal domain antibody antigen-binding fragment inhibits PCSK9 internalization and restores low density lipoprotein uptake. *J. Biol. Chem.* **285,** 12882–12891
45. Zhang, Y., Zhou, L., Beltran, M. K., Li, W., Moran, P., Wang, J., Quan, C., Tom, J., Kolumam, G., Elliott, J. M., Skelton, N., Peterson, A., and Kirchhofer, D. (2012) Calcium-independent inhibition of PCSK9 by affinity-improved variants of the LDL receptor EGF(A) domain. *J. Mol. Biol.*, in press
46. Mayer, G., Poirier, S., and Seidah, N. G. (2008) Annexin A2 is a C-terminal PCSK9-binding protein that regulates endogenous low density lipoprotein receptor levels. *J. Biol. Chem.* **283,** 31791–31801
47. Seidah N. G., Poirier, S., Denis, M., Parker, R., Miao, B., Mapelli, C., Prat A, Wassef, H., Davignon, J., Hajjar, K. A., and Mayer, G. (2012) Annexin A2 is a natural extrahepatic inhibitor of the PCSK9-induced LDL receptor degradation. *PLoS One* **7,** e41865
48. Geoghegan, K. F., Hoth, L. R., Varghese, A. H., Lin, W., Boyd, J. G., and Griffor, M. C. (2009) Binding to low-density lipoprotein receptor accelerates futile catalytic cycling in PCSK9 and raises the equilibrium level of intramolecular acylenzyme. *Biochemistry* **48,** 2941–2949
49. Cariou, B., Ouguerram, K., Zaïr, Y., Guerois, R., Langhi, C., Kourimate, S., Benoit, I., Le May, C., Gayet, C., Belabbas, K., Dufernez, F., Chétiveaux, M., Tarugi, P., Krempf, M., Benlian, P., and Costet, P. (2009) PCSK9 dominant negative mutant results in increased LDL catabolic rate and familial hypobetalipoproteinemia. *Arterioscler. Thromb. Vasc. Biol.* **29,** 2191–2197
50. Abifadel, M., Rabès, J. P., Devillers, M., Munnich, A., Erlich, D., Junien, C., Varret, M., and Boileau, C. (2009) Mutations and polymorphisms in the proprotein convertase subtilisin kexin 9 (PCSK9) gene in cholesterol metabolism and disease. *Hum. Mutat.* **30,** 520–529
51. Abifadel, M., Guerin, M., Benjannet, S., Rabès, J. P., Le Goff, W., Julia, Z., Hamelin, J., Carreau, V., Varret, M., Bruckert, E., Tosolini, L., Meilhac, O., Couvert, P., Bonnefont-Rousselot, D., Chapman, J., Carrié, A., Michel, J. B., Prat, A., Seidah, N. G., and Boileau, C. (2012) Identification and characterization of new gain-of-function mutations in the PCSK9 gene responsible for autosomal dominant hypercholesterolemia. *Atherosclerosis* **223,** 394–400
52. Sun, X. M., Eden, E. R., Tosi, I., Neuwirth, C. K., Wile, D., Naoumova, R. P., and Soutar, A. K. (2005) Evidence for effect of mutant PCSK9 on apolipoprotein B secretion as the cause of unusually severe dominant hypercholesterolaemia. *Hum. Mol. Genet.* **14,** 1161–1169
53. McNutt, M. C., Kwon, H. J., Chen, C., Chen, J. R., Horton, J. D., and Lagace, T. A. (2009) Antagonism of secreted PCSK9 increases low-density lipoprotein receptor expression in HEPG2 cells. *J. Biol. Chem.* **284,** 10561–10570